TABLE I

Transistor	Mitsubishi MGF1412 GASFET	Fujitsu FHR01FH HEMT
Reference	[12]	[13]
Temperature	15 K	12.5 K
Frequency	1.6 GHz	8.4 GHz
T_{min}	7.4 K	10.3 K
$4NT_0$	16.0 K	13.9 K
$-T_{neg}$	8.6 K	3.6 K
R_{opt}	50	4.6
X_{opt}	0	17.0

REFERENCES

[1] J. R. Tucker and M. J. Feldman, "Quantum detection at millimeter wavelengths," *Rev. Mod. Phys.*, vol. 57, no. 4, Oct. 1985.

[2] L. R. D'Addario, "An SIS mixer for 90–120 GHz with gain and wide bandwidth," *Int. J. Infrared and Millimeter Waves*, vol. 5, pp. 1419–1422, 1984.

[3] S-K. Pan, M. J. Feldman, A. R. Kerr, and P. Timbie, "Low-noise, 115 GHz receiver using superconducting tunnel junctions," *Appl Phys. Lett.*, vol. 43, no 8, pp. 786–788, Oct. 15, 1983.

[4] D. W. Face, D. E. Prober, W. R. McGrath, and P. L. Richards, "High-quality tantalum superconducting tunnel junctions for microwave mixing in the quantum limit," *Appl. Phys. Lett.*, vol. 48, no 16, pp. 1098–1100, Apr. 21, 1986.

[5] A. R. Kerr, private communication, Feb. 17, 1987.

[6] M. W. Pospieszalski, "On the noise parameters of isolator and receiver with isolator at the input," *IEEE Trans. Microwave Theory Tech.*, vol. MTT-34, pp. 451–453, Apr. 1986.

[7] H. T. Friis, "Noise figures of radio receivers," *Proc. IRE*, vol. 32, pp. 419–422, July 1944.

[8] H. A. Haus, and R. B. Adler, "An extension of the noise figure definition," *Proc. IRE*, vol. 45, pp 690–691, May 1957.

[9] H. A Haus and R. B. Adler, "Optimum noise performance of linear amplifiers," *Proc. IRE*, vol. 46, pp. 1517–1533, Aug. 1958

[10] H Rothe and W. Dahlke, "Theory of noisy four-poles," *Proc. IRE*, vol. 44, pp. 811–818, June 1956.

[11] R. P. Meys, "A wave approach to the noise properties of linear microwave devices," *IEEE Trans. Microwave Theory Tech.*, vol. MTT-26, pp. 34–37, Jan. 1978.

[12] S. Weinreb, "Noise parameters of NRAO 1 5 GHz GASFET amplifiers," Electronics Division Internal Report No. 231, National Radio Astronomy Observatory, Charlottesville, VA, Dec. 1982.

[13] M. Pospieszalski and S. Weinreb, "FET's and HEMT's at cryogenic temperatures—Their properties and use in low-noise amplifiers," in *1987 IEEE MTT-S Int. Microwave Symp. Dig.*, vol. II (Las Vegas, NV), June 1987, pp. 955–958.

[14] S. Weinreb, D. L. Fenstermacher, and R. W Harris, "Ultra-low-noise 1.2- to 1.7-GHz cooled GaAs FET amplifiers," *IEEE Trans. Microwave Theory Tech.*, vol MTT-30, pp. 849–853, June 1982.

Plotting Vector Fields with a Personal Computer

DARKO KAJFEZ, SENIOR MEMBER, IEEE, AND
JAMES A. GERALD, STUDENT MEMBER, IEEE

***Abstract*—A combination of a personal computer and an $x-y$ plotter is utilized for generating high-quality graphical displays of vector fields. The input data file must specify values of the vector field at a number of equidistant points. Starting points of field lines are determined so that the partial fluxes between any two adjacent field lines are made equal to each other. The construction of the field lines proceeds in a two-step method, utilizing the interpolated values of the field data.**

Manuscript received March 18, 1987, revised June 19, 1987. This material is based upon work supported by the National Science Foundation under Grant ECS 8443558.

The authors are with the Department of Electrical Engineering, University of Mississippi, University, MS 38677.

IEEE Log Number 8716597.

I. INTRODUCTION

A graphical display of electric and magnetic vector fields is indispensable for understanding the operation of many microwave devices. This short paper is concerned with the display of vector fields only. Computer programs for plotting the equicontours of scalar fields are already commercially available [1].

Examples of vector-field displays, generated by computer, can be found in recent references [2]–[4]. These references demonstrate that the smooth plots of vector fields can be obtained from discretized numerical data. The same references also demonstrate that a considerable initial programming effort is necessary and that, as a rule, a mainframe computer is required for implementation.

A systematic approach to graphical displaying of vector fields is possible if the program for computation of the field values is separated from the program which generates the field plots. The separation can be accomplished by requiring the field evaluation program to create a file of the vector-field values at a set of equidistant points, and then by devising a program which draws the smooth lines between these points. Such a general-purpose plotting program, reported in [5] and [6], was written for a mainframe computer and, in addition, it required the use of a large-size, general-purpose graphics software. Gradually, it was realized that the same task can be accomplished with considerably more modest equipment, such as a combination of a personal computer and an $x-y$ plotter. Although ordinary monitor displays on personal computers provide a very limited resolution (200 pixels vertically), the actual plotting accuracy is independent of the screen resolution. Even the modest $x-y$ plotters provide an excellent resolution of 0.025 mm [7]. Therefore, the personal computer can generate plots of a quality equal to those generated by mainframe computers and related hardware.

An algorithm for plotting the field lines and a procedure for selecting the starting points will be described, so that the density of field lines becomes a measure of the intensity of the vector field. The procedure is well suited for implementation on personal computers.

II. CONSTRUCTION OF FIELD LINES

The field lines are plotted in a plane, described in terms of Cartesian coordinates x and y. In the case of an electric field, the components are denoted E_x and E_y:

$$\boldsymbol{E}(x,y) = \hat{x}E_x(x,y) + \hat{y}E_y(x,y). \tag{1}$$

For time-harmonic fields, $\boldsymbol{E}$ is complex, and the instantaneous (real) value of the field must be computed by taking the real part of the expression $\boldsymbol{E}(x,y)\exp(j\omega t)$. Each component of the vector field is assumed to be a quasi-linear function of position, for instance,

$$E_x(x,y) = C_1x + C_2y + C_3 + C_4xy. \tag{2}$$

The four coefficients C_1 to C_4 can be computed from the known field values at the four corner points of an individual cell in a grid of equidistant data points.

The inclination angle θ of the field vector $\boldsymbol{E}$ is specified by

$$\tan\theta = E_y/E_x. \tag{3}$$

Vector fields are represented by continuous field lines, also called lines of force [8, p. 161]. The line of force is tangential to the direction of the vector to be plotted. The differential equation

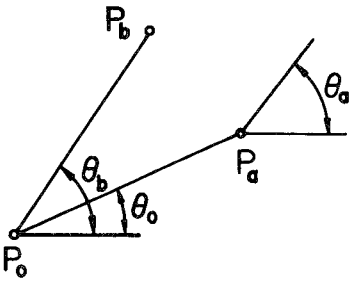

Fig 1 Two-step construction of the field line

for the field line is

$$dy/dx = \tan\theta(x, y). \tag{4}$$

The solution of (4) is the equation of the required field line:

$$y = y(x). \tag{5}$$

A convenient two-step procedure for constructing the small increment of a field line is illustrated in Fig. 1. Suppose the starting point is P_0. The value of the slope at this point is denoted θ_0. First, a trial step of the length s_L is made in the direction θ_0. The corresponding trial point is denoted P_a. At this point, the slope value is θ_a. The average value of the two slopes is

$$\theta_b = (\theta_0 + \theta_a)/2. \tag{6}$$

Starting again from the point P_0, the second step is made in the direction θ_b, using the same step length s_L. The resulting point is denoted P_b. Afterwards, P_b is used as a starting point, and the same two-step procedure is repeated. The procedure resembles the second-order Runge–Kutta method [9, eq. (6.15.15)]. It can be shown that the algorithm accurately represents the second-order term in the power expansion of the differential equation (4).

It may be possible to further increase the accuracy of the algorithm, at the expense of its simplicity. An alternative, and at the same time graphically more pleasing, way of increasing the accuracy of the field lines is to reduce the step size s_L. It appears that the compromise between satisfying accuracy and reasonable execution times is obtained when s_L is between 1/40th and 1/80th of the diagonal of the total plot size. No numerical instabilities have been observed when s_L was reduced to values even ten times smaller.

The piecewise construction of the field lines is interrupted when one of the stopping criteria is violated. The most obvious reason for stopping is that the line has reached the boundary of the area to be covered. Another reason is that the line has completed a closed loop and returned to the starting point. A third reason is that the field magnitude has dropped below a prescribed level (say, 1 percent to 5 percent of the maximum magnitude). Finally, the plotting of the field line should be stopped when a singular point is approached (a point at which the field magnitude tends to infinity).

III. Selection of Starting Points

Starting from any point in the plotting area, the algorithm described in the previous section makes it possible to draw continuous field lines. The starting points must be selected in a systematic way, so that the density of the field lines becomes a measure of the field strength in the region under consideration. This can be achieved by ascertaining that all partial fluxes between any two adjacent field lines are made equal to each other.

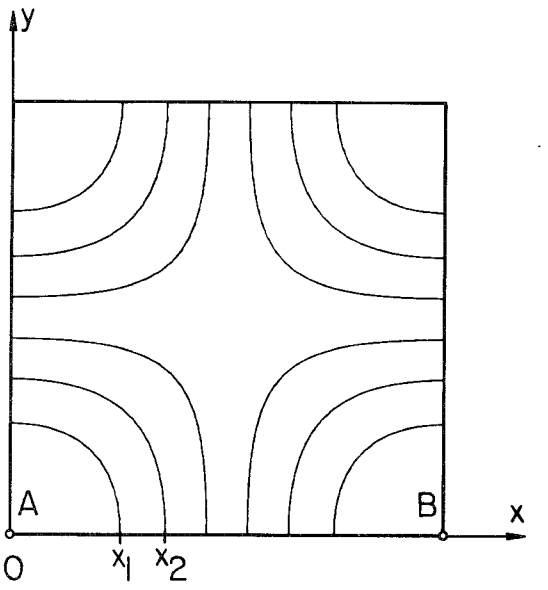

Fig 2 Computing the position of starting points on the flux intercept line $\overline{AB}$.

Fig. 2 displays the electric field of the TE_{11} mode in a rectangular waveguide. The bottom surface of the waveguide is selected to coincide with the x coordinate. For the waveguide of width a, the total flux of the electric field between points A and B is

$$\psi = \int_{x=0}^{a} E_y(x)\, dx. \tag{7}$$

This total flux must be divided into an integral number of partial fluxes. For instance, if the number of field lines starting from the waveguide wall $\overline{AB}$ is M, then the partial flux should be

$$\Delta\psi = \frac{\psi}{M+1}. \tag{8}$$

In order to find the first starting point x_1, the value of x_1 must be found such that

$$\int_0^{x_1} E_y(x)\, dx = \Delta\psi. \tag{9}$$

After determining position x_1, an integration over the next interval is performed to find point x_2, etc. A total of M starting points are determined in this manner. The integrals are evaluated numerically, by interpolating between the known data points with the use of (2).

It can be seen that the intercept line on the bottom wall of the rectangular waveguide in Fig. 2 provides the starting points for only one half of the total number of field lines. When this figure was plotted, another intercept line was placed on the top wall of the waveguide, to furnish the starting points of the remaining field lines.

All the electric field lines in Fig. 2 start perpendicularly from the boundary lines (metal walls in this case). The magnetic field lines are of a different nature, typically forming closed loops, as for instance in the TM_{11} waveguide field shown in Fig. 3. The starting points for plotting the magnetic field lines should be again selected on a straight line which is perpendicular to field lines. A convenient choice is a "flux intercept line" $\overline{CD}$ in Fig. 3.

In more complicated field distributions, several flux intercept lines should be placed at different positions in the figure, in order to intercept all possible field lines. Some *a priori* knowledge of the field distribution is required for choosing the position of flux

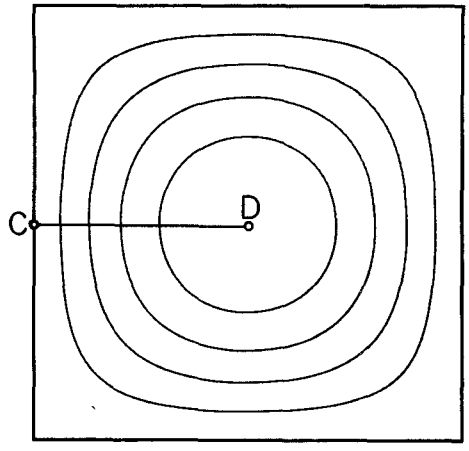

Fig. 3. Flux intercept line $\overline{CD}$ which is not located on the boundary.

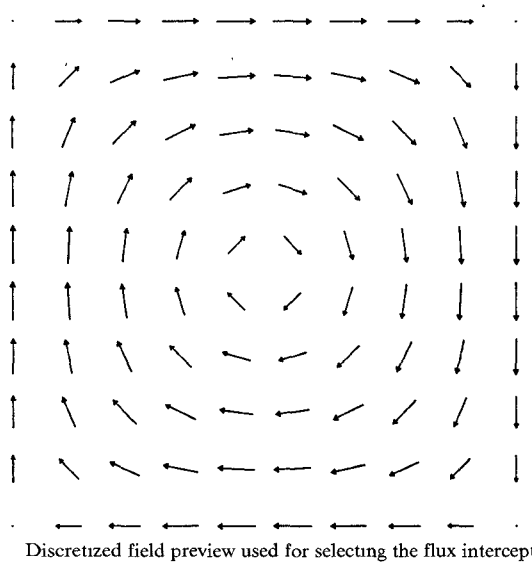

Fig 4 Discretized field preview used for selecting the flux intercept line.

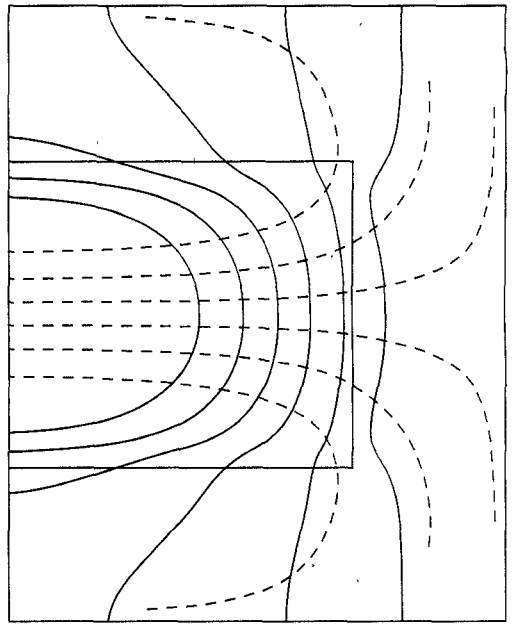

Fig 5. Electric field (solid lines) and magnetic field (dashed lines) of the HEM_{12} mode in a shielded dielectric resonator.

intercept lines. Consequently, plotting of the field with a computer must be performed in an interactive manner, so that certain decisions are made only after some computations have been completed and partial results graphically displayed on the computer monitor. A convenient intermediate display of the field is the discretized preview of the input data file. At the location of each data point, a small arrow is drawn in the direction of the field vector, as in Fig. 4, which is an actual 10×10 data file used to plot Fig. 3. In the interactive mode, it is convenient to enter the position of the end points of the intercept lines with the cursor keys which control the horizontal and vertical movement on the screen.

IV. Implementation on Personal Computer

The disk operating system (DOS) of the IBM personal computer comes with the BASICA language [10]. This language is adequate for all the computations involved in generating the field plots, and it also comprises convenient commands for the graphic display on the computer monitor. The program described here has been originally developed in this language. Later, it was found that the execution speed can be greatly increased by using a compiled Basic software, called QUICK BASIC [11]. Significant increase in the speed of computation can further be achieved with the use of the mathematical coprocessor chip 8087. The recently released software TURBO BASIC [12] accomplishes this goal very well while still being entirely compatible with the BASICA language, including all graphics commands.

The program performs the following operations: it provides the discretized preview of the field in order to allow the selection of the flux intercept lines, it displays the field lines on the monitor, and it plots the field lines on the $x-y$ plotter.

Fig. 5 shows the electric and magnetic fields of the HEM_{12} mode in a shielded dielectric resonator. The field values have been computed by the finite integration technique (FIT) on a grid of 17×14 points. These data were provided by courtesy of J. Lebaric. Since the field is rotationally symmetric, only one half of the cross section is shown.

V. Summary

Quality plotting of electric and magnetic field lines used to be restricted to the mainframe computers and associated graphics hardware. Nowadays, the numerical solution of practical electromagnetic boundary value problems still requires the use of the mainframe computer. However, the resulting data file for the field distribution can be conveniently studied on the screen of a small personal computer, and eventually plotted, with great precision, on a relatively inexpensive $x-y$ plotter. The software which allows such an interactive display and plotting has been devised using the principles presented in this short paper.

References

[1] *SAS/Graph User's Guide*, SAS Institute Inc., Cary, NC, 1981, p. 43.
[2] C. S. Lee, S. W. Lee, and S. L. Chang, "Plot of modal field distribution in rectangular and circular waveguides," *IEEE Trans Microwave Theory Tech.*, vol. MTT-33, pp. 271–274, Mar. 1985.
[3] P. E. Moller and R. H. McPhie, "On the graphical representation of electric field lines in waveguide," *IEEE Trans. Microwave Theory Tech.*, vol. MTT-33, pp. 187–192, Mar. 1985.
[4] K. A. Zaki and C. Chen, "Intensity and distribution of hybrid-mode fields in dielectric-loaded waveguides," *IEEE Trans. Microwave Theory Tech.*, vol. MTT-33, pp. 1442–1447, Dec. 1985.
[5] D. Kajfez and R. T. Ward, "Computer program for plotting the vector fields," in *Abstracts of 1986 Nat. Radio Sci. Meeting* (Philadelphia), June 8–13, 1986, p. 200.
[6] D. Kajfez and R. T. Ward, "Plotting of two-dimensional vector fields with computer," Dept. of Electrical Engineering, University of Mississippi, NTIS accession no. PB86-196318, Apr 1986.

[7] *Electronic Measurement, Design, Computation*, Hewlett Packard Co., Palo Alto, CA, 1987, p. 110.
[8] J. A Stratton, *Electromagnetic Theory*. New York: McGraw-Hill, 1941.
[9] F. B Hildebrand, *Introduction to Numerical Analysis*. New York: McGraw-Hill, 1956
[10] *Basic by Microsoft Corp*, IBM Personal Computer Hardware Reference Library, 1982
[11] *Microsoft Quick Basic Compiler*, Microsoft Corp., Redmond, WA, 1986.
[12] *Turbo Basic Owner's Handbook*, Borland International, Scotts Valley, CA, 1987.

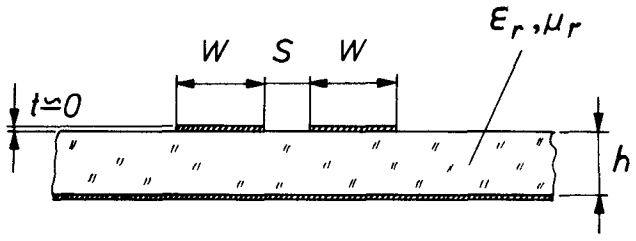

Fig. 1. Transverse section of the coupled microstrip lines.

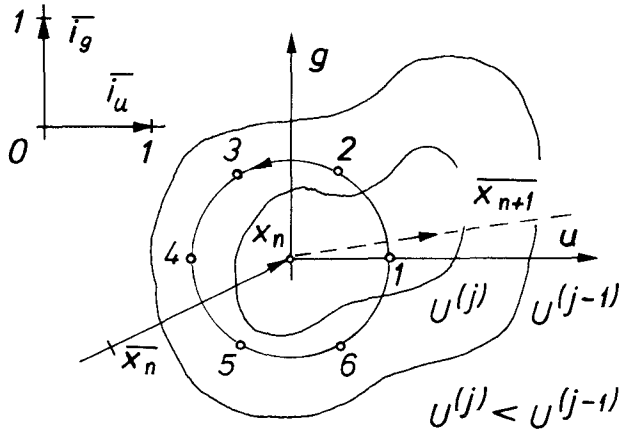

Fig. 2. Diagram of the search process.

Design of Coupled Microstrip Lines by Optimization Methods

STANISŁAW ROSŁONIEC

Abstract—**The design of two coupled microstrip lines is converted into an optimization problem, which is then solved by two methods of nonlinear mathematical programming. New formulas for calculating the first approximation of the solution, i.e., the starting point of the optimization, are given.**

I. Introduction

The design of two parallel coupled microstrip lines has been extensively studied in the literature (see e.g. [1]–[9]). The formulas given in [7] and [8] are most useful for accuracy reasons. They make it possible to calculate the line impedances Z_{0e} and Z_{0o} provided the geometric dimensions and the permittivity of the dielectric substrate are given. In practice, the reverse problem is usually solved, which is equivalent to the problem of solving two nonlinear equations with strip width and slot width as variables. An algorithm for solving this set of equations should be reliable, accurate, and quickly convergent. In this paper the design problem of two coupled microstrip lines is converted into an optimization problem, which is then solved by two methods of nonlinear mathematical programming, applied subsequently when approaching the solution. New formulas for calculating the first approximation of the solution being sought, i.e., the starting point for the optimization, are given. Properties of the design algorithm are illustrated by calculated results.

II. The Design Algorithm

A transverse section of the coupled lines being considered is shown in Fig. 1. If $u = W/h$ and $g = S/h$, the characteristic impedances Z_{0e} and Z_{0o} of these lines can be expressed as

$$Z_{0e} = F_1(u, g, \epsilon_r)$$
$$Z_{0o} = F_2(u, g, \epsilon_r) \tag{1}$$

where F_1 and F_2 are relations given in the papers cited above, e.g., [7]. The problem of designing two coupled microstrip lines for given impedances Z_{0e}, Z_{0o} and permittivity ϵ_r of a dielectric substrate consists of determination of the values u_S and g_S

$$F_1(u_S, g_S, \epsilon_r) - Z_{0e} = 0$$
$$F_2(u_S, g_S, \epsilon_r) - Z_{0o} = 0. \tag{2}$$

Manuscript received March 30, 1987; revised June 19, 1987.
The author is with the Institute of Radioelectronics, Warsaw Technical University, 00-665 Warsaw, Nowowiejska 15/19, Poland.
IEEE Log Number 8716600

It can easily be seen that solution of (2) is equivalent to finding a global minimum of the following function:

$$U(u, g, \epsilon_r) = [F_1(u, g, \epsilon_r) - Z_{0e}]^2 + [F_2(u, g, \epsilon_r) - Z_{0o}]^2. \tag{3}$$

From (2) it is evident that function (3) reaches its global minimum equal to zero at the point being sought (u_S, g_S). According to (3) the problem being considered can be written in the form

$$\min_{(u,g) \subset D} U(u, g, \epsilon_r) \tag{4}$$

where D is the set of values of u and g possible from the point of view of the construction. The above-formulated minimization problem has been solved by various methods of nonlinear mathematical programming, i.e., the steepest descent, Fletcher–Reeves, and Davidon–Fletcher–Powell methods [10].

From the performed analysis it is seen that the best results, in the sense of the criterion given earlier, are ensured by the Davidon–Fletcher–Powell method and the direct nongradient search. In the prepared subroutine, entitled "coupled lines" (see next page), the direct search is conducted at six points lying on a circle (Fig. 2) with radius $h_n/2$ [9]. Function (3) takes its minimal value, while searching in direction $\bar{x}_n$ with the step h_n, at point x_n, which is the center of this circle. This nongradient method is additionally used when $U(u, g, \epsilon_r) < 3$. The search terminates if $U(u, g, \epsilon_r) < Z_{0e} \cdot Z_{0o}/10000$, which ensures a relative approximation accuracy not worse than 1 percent for the impedances.

The reasonable choice of the first approximation, i.e., the starting point for optimization, significantly affects the computation time. In the coupled lines subroutine, the first approximation is found according to the formula [9]

$$u_0 = |F_3(Z_0, \epsilon_r) \cdot F_4(k)|$$
$$g_0 = |F_3(Z_0, \epsilon_r) \cdot F_5(k, \epsilon_r)| \tag{5}$$

0018-9480/87/1100-1072$01.00 ©1987 IEEE